Available online at www.sciencedirect.com
SCIENCE DIRECT®
Journal of Computational Physics 207 (2005) 375–387
JOURNAL OF COMPUTATIONAL PHYSICS
www.elsevier.com/locate/jcp

Computation of eigenmodes of photonic crystals by inversion of the Maxwell operator

François Delyon, Michel Duneau *

Centre de Physique Théorique, CNRS, UMR 7644, Ecole Polytechnique 91128 Palaiseau, Cedex, France

Received 3 November 2004; received in revised form 18 January 2005; accepted 24 January 2005
Available online 14 March 2005

Abstract

We describe a method to compute the lowest eigenvalues of the Maxwell operator in a periodic medium. We prove that the Lánczos method applied to the inverse Maxwell operator provides a fast, robust and superconvergent algorithm. We apply this method to the computation of the dispersion relations of a 2D photonic crystal.

Keywords: Photonic crystal; Photonic band gap; Maxwell operator; Lánczos method; Compact operator

1. Introduction

Since Yablonovitch's pioneering work [1] there has been considerable work in the investigation of the optical properties of two- and three-dimensional (2D and 3D) photonic crystals. These media are expected to provide new devices with functionalities similar to those obtained with current electronic devices. Electronic band gaps in semi conductors may have their counterpart in photonic crystals if these new structures exhibit photonic band gaps, i.e., if there exist frequencies for which the propagation of light is impossible.

Whereas the crystalline periodicity of semiconductors yields electronic band gaps which readily fit with most electronic applications, photonic crystals with periodicity of order 1 μm have to be constructed. Computer softwares are therefore needed to simulate their properties, depending on the lattice symmetry and on the distribution of the refractive index.

* Corresponding author. Tel.: +33 1 69334730; fax: +33 1 69333008.
E-mail address: duneau@cpht.polytechnique.fr (M. Duneau).

0021-9991/$ - see front matter
doi:10.1016/j.jcp.2005.01.015

Photonic gaps are expected to occur only in the lower part of the frequency spectrum of the eigenmodes. It is therefore necessary to compute the first modes of the stationary Maxwell equations in a periodic medium. This leads to an eigenvalue problem involving the so-called Maxwell operator. The periodicity of the permittivity allows to reduce the equations in a form similar to the Bloch equations for electrons in a periodic potential. For each Bloch vector k one gets an eigenvalue problem in the unit cell with particular boundary conditions which yields a discrete sequence of eigenvalues depending continuously on k. When k runs over the Brillouin zone these eigenvalues fill up closed intervals of the positive real axis and the complete spectrum is the union of these intervals. Photonic band gap occur when the spectrum does not cover the positive axis.

The lowest eigenvalues of a symmetric operator can be computed by different methods: the Lánczos method and the Rayleigh quotient method for instance (see [2–6]). The well-known MIT Photonic-Bands (MPB) package is based on the Rayleigh quotient method [7]. However, these algorithms are difficult to control in the case of the Maxwell operator because its spectrum is not bounded: for each Bloch vector k the sequence of eigenvalues tends to infinity. This raises delicate questions as regards to the convergence of the computed eigenvalues and eigenvectors.

This work is part of a project intended to develop an holographic method for a direct growth of 2D and 3D photonic crystals by chemical vapor deposition. The project is presented in [8] where an experimental setup is described.

In this article, we concentrate on the theoretical and computational aspects linked to the description of the eigenmodes in a 2D or 3D periodic photonic crystal. We present a method based on the iteration of the inverse Maxwell operator. This inverse operator is bounded (more precisely compact) and it turns out that estimates on the convergence of its largest eigenvalues can easily be obtained. The mere drawback of this method relies in the inversion of the Maxwell operator which, however, can be handled without much difficulty. The advantage is that this method leads to fast computations: for instance the nth first modes require about $4n$ inverse Maxwell operator.

This article is organized as follows: in Section 2, we recall the mathematical framework of Maxwell equations in a non-magnetic periodic medium. In Section 3, we introduce the method based on the iteration of the inverse Maxwell operator. We discuss the convergence of the eigenvalues with respect to the number of iterations which corresponds to the dimension of the Krylov space generated by the algorithm. In Section 4, we present and we discuss numerical results obtained in the case of a 2D honeycomb photonic crystal.

2. Maxwell equations in a periodic medium

2.1. The Maxwell operator for dielectrics

If the charge density is null and if the system is not magnetic the Maxwell equations for time periodic solutions reduce to the differential system

$$\nabla \times (\varepsilon^{-1} \nabla \times H) = \frac{\omega^2}{c^2} H, \tag{1}$$

$$\nabla \cdot H = 0, \tag{2}$$

where $H : \mathbb{R}^3 \to \mathbb{C}^3$ is the complex magnetic field (H_x, H_y, H_z), ε is the permittivity and ω is the pulsation.

Let $\mathscr{H}$ denote the Hilbert space of magnetic fields with the norm

$$\int_{\mathbb{R}^3} (|H_x|^2 + |H_y|^2 + |H_z|^2)\,\mathrm{d}v.$$

Then $\mathscr{H}$ can be split as a direct sum $\mathscr{H} = \mathscr{H}_\parallel \oplus \mathscr{H}_\perp$ with

$$\mathscr{H}_\parallel = \{H \in \mathscr{H} : k \times \widetilde{H}(k) = 0 \text{ a.e.}\},$$
$$\mathscr{H}_\perp = \{H \in \mathscr{H} : k \cdot \widetilde{H}(k) = 0 \text{ a.e.}\},$$

where $H(x) = \int \mathrm{e}^{\imath kx}\widetilde{H}(k)$ and $\mathscr{H}_\perp$ is the subspace of transverse fields which satisfy the transversality condition (2).

Let $\mathscr{H}_0 \subset \mathscr{H}$ denote the dense subspace of magnetic fields with square integrable first and second derivatives. Following the above decomposition of $\mathscr{H}$, we have the direct sum $\mathscr{H}_0 = \mathscr{H}_{0,\parallel} \oplus \mathscr{H}_{0,\perp}$.

The curl operator $\nabla\times$ is essentially self-adjoint on $\mathscr{H}_0$. Its kernel is $\mathscr{H}_{0,\parallel}$ and its range is dense in $\mathscr{H}_\perp$. Thus, $\nabla\times$ is essentially self-adjoint on $\mathscr{H}_{0,\perp}$.

In the differential systems (1) and (2), the operator ε^{-1} sandwiched between two curl operators can be replaced by $P_\perp\varepsilon^{-1}P_\perp$ where $P_\perp$ is the orthogonal projector on $\mathscr{H}_\perp$.

Consequently, the differential system can be understood as the eigenvalue problem associated to the Maxwell operator

$$\boldsymbol{\Theta} = \nabla \times P_\perp\varepsilon^{-1}P_\perp\nabla\times, \tag{3}$$

which is essentially self-adjoint and positive on $\mathscr{H}_{0,\perp}$.

This construction is straightforward for sufficiently regular ε and can be readily extended to positive discontinuous ε.

2.2. The Maxwell operator in periodic media

We assume now that ε is periodic with respect to a three-dimensional lattice L and that $\varepsilon(x) \in [\varepsilon_1, \varepsilon_2]$ with $0 < \varepsilon_1 \leqslant \varepsilon_2 < \infty$.

The dual lattice is denoted L^* and B is the Brillouin zone in reciprocal space. The Hilbert space $\mathscr{H}$ can be decomposed as a continuous sum of Hilbert spaces [9]

$$\mathscr{H} \equiv \int_B^\oplus \mathscr{H}(k)\,\mathrm{d}k, \tag{4}$$

where each Hilbert space $\mathscr{H}(k)$ is the space of L-periodic magnetic fields. The corresponding Block decomposition of a field $H \in \mathscr{H}$ is given by

$$H(x) = \int_B \mathrm{d}k\,\mathrm{e}^{\imath kx}h_k(x),$$

where

$$h_k(x) = \sum_{Q\in L^*} \mathrm{e}^{\imath Q\cdot x}\widetilde{H}(k+Q) = \frac{V}{(2\pi)^3}\sum_{t\in L}\mathrm{e}^{-\imath k(x+t)}H(x+t).$$

V is the volume of the unit cell of L and the fields h_k are L-periodic.

The Hermitian product in $\mathscr{H}$ may be expressed as follows:

$$(H', H) = \int_B \mathrm{d}k(h'_k, h_k),$$
$$(h'_k, h_k) = \int_{\text{U.C.}} \mathrm{d}x(h'_k(x), h_k(x)).$$

Similarly, the Hilbert space $\mathscr{H}_\perp$ can be decomposed as

$$\mathscr{H}_\perp \equiv \int_B^\oplus \mathscr{H}_\perp(k)\,\mathrm{d}k, \tag{5}$$

where each Hilbert space $\mathscr{H}_\perp(k)$ is the space of L-periodic magnetic fields $h_k(x) = \sum_Q \mathrm{e}^{\imath Qx} h_{k,Q}$ whose Fourier components satisfy the transversality condition

$$(k+Q)\cdot h_{k,Q} = 0 \quad \forall Q \in L^*.$$

The curl operator $\nabla\times$ can be decomposed by the direct integral decomposition (5)

$$\begin{aligned} \nabla\times &= \int_B^\oplus \mathbf{B}_k\,\mathrm{d}k, \\ (\mathbf{B}_k h_k)_Q &= \imath(k+Q)\times h_{k,Q} \quad \forall Q \in L^*. \end{aligned} \tag{6}$$

Thus, the Fourier components $h_{k,Q}$ are scaled by $\imath|k+Q|$ and rotated by $\pi/2$ in the polarization plane orthogonal to $k+Q$. The corresponding eigenvalues of $\mathbf{B}_k$ are therefore $\pm|k+Q|$ for $Q \in L^*$. Then the spectrum of $\mathbf{B}_k$ is isolated from 0 if $k \neq 0$.

The operator $P_\perp \varepsilon^{-1} P_\perp$ can be decomposed by the direct integral (5)

$$P_\perp \varepsilon^{-1} P_\perp = \int_B^\oplus \mathbf{A}_k\,\mathrm{d}k$$

where $\mathbf{A}_k$ is the multiplication by ε^{-1} followed by the projection $P_{\perp,k}$ onto $\mathscr{H}_\perp(k)$, i.e.

$$(P_{\perp,k}h)_Q = h_Q - \frac{(k+Q,h_Q)}{(k+Q,k+Q)}(k+Q). \tag{7}$$

The Maxwell operator $\boldsymbol{\Theta}$ is thus decomposed as

$$\boldsymbol{\Theta} = \int_B^\oplus \boldsymbol{\Theta}_k\,\mathrm{d}k = \int_B^\oplus \mathbf{B}_k\mathbf{A}_k\mathbf{B}_k\,\mathrm{d}k. \tag{8}$$

2.3. The eigenvalue problem

The spectrum of $\boldsymbol{\Theta}$ is the union of the spectra of the $\boldsymbol{\Theta}_k$'s for $k \in B$. The operators $\mathbf{B}_k$ have compact inverse for $k \neq 0$ as follows from Eq. (6) (for $k = 0$ this remains true since we restrict $\mathbf{B}_0$ to the orthogonal of its obvious kernel). The operators $\mathbf{A}_k$'s are strictly positive ($0 < \varepsilon_1 \leqslant \mathbf{A}_k \leqslant \varepsilon_2 < \infty$). Thus, $\boldsymbol{\Theta}_k^{-1}$ is compact as product of compact and bounded operators. Its spectrum is a set of isolated positive eigenvalues $\omega^2_i(k)c^{-2}$ (with finite multiplicity) with $\omega^2_i(k) \to \infty$ as $i \to \infty$. Furthermore, these operators are norm-continuous (in the resolvent sense) with respect to k. Thus, the spectrum of $\boldsymbol{\Theta}$ is the countable union $S = \cup_i b_i$ of the bands $b_i = \cup_{k\in B}\ \omega^2_i(k)c^{-2}$. Gaps are open if these bands do not cover the whole positive line $\mathbb{R}^+$.

One expects the bands to overlap for large frequencies so that the opening of gaps only concerns the lower part of the spectrum. The gap problem reduces to solving the eigenvalue equation

$$\mathbf{B}_k\mathbf{A}_k\mathbf{B}_k h_i = \frac{\omega_i^2(k)}{c^2} h_i, \tag{9}$$

for the few first i corresponding to the lowest eigenvalues.

2.4. The 2D Maxwell problem

One may consider particular cases where ε is invariant along the z-axis and is periodic in the horizontal plane. The translation lattice L and the reciprocal lattice L^* are two dimensional. In this case, the 3D Maxwell operator cannot have gaps and the spectrum is $\mathbb{R}^+$.

However, it makes sense to consider the propagation parallel to the horizontal plane ($k_z = 0$). In this case, the operators $\mathbf{B}_k\mathbf{A}_k\mathbf{B}_k$ preserve the two subspaces TE ($h_k = (0,0,h_z)$) and TM ($h_k = (h_x,h_y,0)$, $(k+Q)\cdot h_{k,Q} = 0$). In either cases and for each $Q \in L^*$, the polarization $h_{k,Q}$ is one dimensional.

Furthermore, in the TM mode, the vectors $\mathbf{B}_k h_k$ are parallel to the z-axis. The vectors $\varepsilon^{-1}\mathbf{B}_k h_k$ are still parallel to the z-axis and thus automatically satisfy the transversality condition. Thus, the Maxwell operators for TM modes may be rewritten as

$$\boldsymbol{\Theta}_k = \mathbf{B}_k \varepsilon^{-1} \mathbf{B}_k. \tag{10}$$

3. Numerical framework

3.1. The inverse Maxwell operator

As shown by (6) the operators $\mathbf{B}_k$ are almost diagonal in the Fourier representation $h_{k,Q}$. On the other hand, the operator ε^{-1} is diagonal in direct space.

As in previous works [7], we solve the eigenvalue problem in Fourier space. The operator ε^{-1} is implemented as the product of an inverse FFT, a diagonal multiplication and a direct FFT. This provides a fast algorithm to compute the action of $\boldsymbol{\Theta}_k$'s avoiding a matrix representation. This allows to handle 3D cases of size of order $100 \times 100 \times 100$.

The problem is to find an efficient algorithm to compute the lowest eigenvalues (and eigenvectors) of the $\boldsymbol{\Theta}_k$'s.

The operator $\boldsymbol{\Theta}_k$ has compact resolvent, and except for $k = 0$, the inverse operator $\boldsymbol{\Theta}_k^{-1} = \mathbf{B}_k^{-1}\mathbf{A}_k^{-1}\mathbf{B}_k^{-1}$ is compact. The goal now is to compute the largest eigenvalues of $\boldsymbol{\Theta}_k^{-1}$. As mentioned above, $\mathbf{B}_k^{-1}$ is easily calculated: for $h \in \mathscr{H}_\perp(k)$ and $k \neq 0$ we have

$$(\mathbf{B}_k^{-1}h)_Q = \frac{\imath}{(k+Q)^2}(k+Q)\times h_Q.$$

For $k = 0$, the subspace $\{h : h_Q = 0, Q \neq 0\}$ is invariant by $\mathbf{B}_0$ and $\boldsymbol{\Theta}_0$. It corresponds to the eigenspace for the trivial eigenvalue 0. On the orthogonal subspace $\{h : h_0 = 0\}$, $\mathbf{B}_0$ has a compact inverse given by

$$(\mathbf{B}_0^{-1}h)_Q = \frac{\imath}{Q^2} Q \times h_Q, \quad (Q \neq 0). \tag{11}$$

However, the computation of the inverse of $\mathbf{A}_k = P_{\perp,k}\varepsilon^{-1}P_{\perp,k}$ requires more attention.

In the case of TM modes (see (10)), ε commutes with $P_{\perp,k}$ and we simply get $\mathbf{A}_k^{-1} = P_{\perp,k}\varepsilon P_{\perp,k} = \varepsilon$.

For TE modes and in the 3D cases, ε does not commute anymore with $P_{\perp,k}$ and $\mathbf{A}_k^{-1} \neq P_{\perp,k}\varepsilon P_{\perp,k}$. Strictly speaking an inverse problem $\mathbf{A}_k x = b$ should be solved at each step of the iteration method presented in the next section. Notice that this inverse problem is regular since the operator $\mathbf{A}_k$ is positive, bounded and satisties $0 < \varepsilon_2^{-1} \leqslant \mathbf{A}_k \leqslant \varepsilon_1^{-1}$. We show in Section 4 that an approximate inverse of $\mathbf{A}_k$ computed by the Conjugate Gradient Method may be used. The accuracy then depends on the number of steps, provided that the $n \times n$ matrix associated to $\boldsymbol{\Theta}_k$ is computed exactly on the approximate Krylov subspace.

3.2. The Lánczos method with compact operators

The Lánczos method [10] is well-suited to compute the largest eigenvalues of a compact symmetric operator. Convergence estimates for the largest eigenvalue of a symmetric matrix can be found for instance in [2]. However, we are also interested in the next few eigenvalues.

The following Theorem gives a posteriori estimates on the convergence of the computed eigenvalues with respect to the dimension of the Krylov space and to the index of the eigenvalue. This theorem can be deduced from Sections 12.4 and 12.5 in [3], we give here a short proof adapted to our context.

Theorem 1. *Let T be a positive symmetric compact operator and let $\lambda_1 > \lambda_2 > \cdots \geqslant 0$ denote the sequence of the distinct eigenvalues of T. Let E_i denote the eigenspace associated to the eigenvalue λ_i and let P_i denote the corresponding projector. Let x denote a unit vector. Then for, $n > p \geqslant 0$ and $1 \leqslant r \leqslant p$, the Krylov subspace $K = \{x, Tx, \ldots, T^{n-1}x\}$ contains a unit vector u_r such that*

$$\|(I - P_r)u_r\| < \tan\varphi_r \delta_r, \tag{12}$$

where

$$\delta_r = \frac{1}{\mathscr{T}_{n-p}(2\lambda_r/\lambda_{p+1} - 1)} \prod_{\substack{i=1 \\ i\neq r}}^{p} \left|\frac{\lambda_i}{\lambda_r - \lambda_i}\right|, \tag{13}$$

$\mathscr{T}_n$ is the nth Tchebichev polynomial and $\varphi_r = \arccos(\|P_r x\|)$.

Proof. Choose $r \in \{1, \ldots, p\}$ and let

$$y = \mathscr{T}_{n-p}(2T/\lambda_{p+1} - 1) \prod_{\substack{i=1 \\ i\neq r}}^{p} (T - \lambda_i)x.$$

Then y belongs to the Krylov space K and satisfies $P_i y = 0$ for $i \in \{1, \ldots, n\}$ and $i \neq r$. If $\mathscr{P}_p = P_1 + \cdots + P_p$ denotes the projector on the subspace $E_1 \oplus \cdots \oplus E_p$ we have

$$\mathscr{P}_p y = \mathscr{T}_{n-p}(2\lambda_r/\lambda_{p+1} - 1) \prod_{\substack{i=1 \\ i\neq r}}^{p} (\lambda_r - \lambda_i)P_r x,$$

$$(I - \mathscr{P}_p)y = \mathscr{T}_{n-p}(2T/\lambda_{p+1} - 1) \prod_{\substack{i=1 \\ i\neq r}}^{p} (T - \lambda_i)(I - \mathscr{P}_p)x.$$

It follows that $\mathscr{P}_p y \in E_r$. We set $\cos\varphi_r = \|P_r x\|$ and $\sin\varphi_r = \|(I - P_r)x\|$ and we get

$$\|\mathscr{P}_p y\| = \cos\varphi_r \, \mathscr{T}_{n-p}(2\lambda_r/\lambda_{p+1} - 1) \prod_{\substack{i=1 \\ i\neq r}}^{p} |\lambda_r - \lambda_i|,$$

$$\|(I - \mathscr{P}_p)y\| \leqslant \sin\varphi_r \prod_{\substack{i=1 \\ i\neq r}}^{p} \lambda_i,$$

since $|\mathscr{T}_{n-p}(x)| \leqslant 1$ on $[-1, 1]$. Then (12) follows with $u_r = y/\|y\|$. □

The following corollary shows that if an eigenvector of T is well approximated in the Krylov space K, then the corresponding eigenvalue is close to an eigenvalue of the $n \times n$ restriction of T to K.

Corollary 1. *With hypotheses and notations of Theorem 1, let P_K denote the projector on the Krylov subspace K and let $T_K = P_K T P_K$. For $1 \leqslant r \leqslant n$, the $n \times n$ operator T_K has an eigenvalue μ such that*

$$|\mu - \lambda_r| \leqslant \lambda_1 \tan\varphi_r \delta_r.$$

Proof. Let u_r be defined as in Theorem 1. Then

$$u_r = v_r + w_r$$

with $\|w_r\| \leqslant \tan\varphi_r\delta_r$ and $Tv_r = \lambda_r v_r$. Then

$$(T_K - \lambda_r)u_r = P_K T u_r - \lambda_r u_r = P_K T w_r + \lambda_r(P_K v_r - u_r) = P_K T w_r - \lambda_r P_K w_r = P_K(T - \lambda_r)w_r.$$

Therefore

$$(u_r, (T_K - \lambda_r)^2 u_r) = \|(T_K - \lambda_r)u_r\|^2 \leqslant \lambda_1^2 \tan^2\varphi_r \delta_r^2.$$

Thus, the operator $(T_K - \lambda_r)^2$ has an eigenvalue bounded by $\lambda_1^2\tan^2\varphi_r\delta_r^2$ and the operator $T_K - \lambda_r$ has an eigenvalue of modulus bounded by $\lambda_1\tan\varphi_r\delta_r$. □

Formula (13), however, is rather complicated and heavily depends on the distribution of eigenvalues. We discuss the behavior of δ_r in the next section.

In order to obtain the band structure of the photonic crystal, we also need to compute the dimensions of the eigenspaces E_r. Strictly speaking, this may be achieved by randomly varying the initial condition x, as long as the resulting eigenvectors are linearly independent. The operator T of Theorem 1 stands for the inverse operator

$$\boldsymbol{\Theta}_k^{-1} = \mathbf{B}_k^{-1}\mathbf{A}_k^{-1}\mathbf{B}_k^{-1},$$

where k is a Block vector in the Brillouin zone. In this case, since degeneracies are expected to be exceptional with respect to k they can be easily identified by continuity.

3.3. Estimates of the convergence in a simple case

We consider now the convergence of the Lánczos method for the operator $T = \boldsymbol{\Theta}_k^{-1}$. In this case, the eigenvalues $\lambda_r \to 0$ as $r \to \infty$ like r^{-2} in 1D, like r^{-1} in 2D and like $r^{-2/3}$ in 3D.

We assume now that $\lambda_r = r^{-1}$. Even in this simple case, the estimation of δ_1 is not obvious

$$\delta_1 = \frac{1}{\mathscr{T}_{n-p}(2p+1)}\,\frac{1}{(p-1)!} \approx \left(\frac{1}{4p}\right)^{n-p}\frac{1}{p^p e^{-p}}.$$

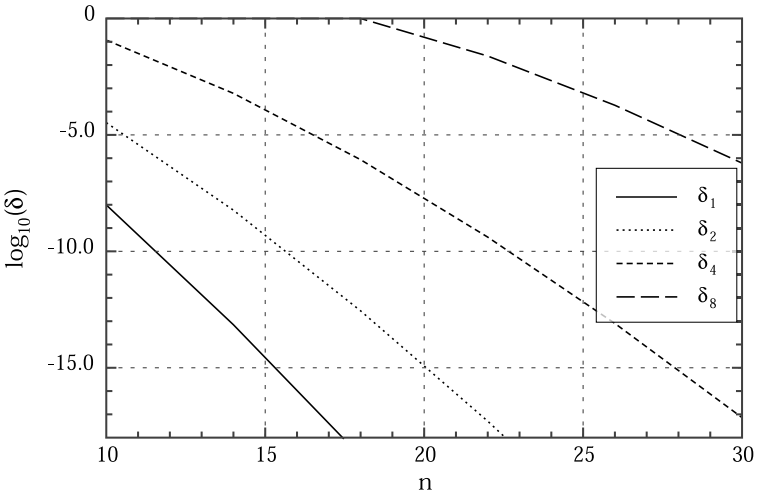

Fig. 1. Upper bounds for δ_1, δ_2, δ_4 and δ_8 as function of the dimension n of the Krylov space for $\lambda_r = 1/r$.

The best estimate of δ_1 is obtained for $p = n/\ln(4e)$ and we get

$$\delta_1 \leqslant \left(\frac{e\ln(4e)}{4n}\right)^n.$$

Therefore, the method is super-convergent with respect to n (for instance $\delta_1 < 10^{-10}$ for $n = 12$).

For subsequent eigenvalues the best estimate for δ_r is complicated. Fig. 1 plots the best p estimates for δ_1, δ_2, δ_4 and δ_8 as function of the dimension n of the Krylov space.

In fact, the asymptotics for large n is not relevant since the accuracy is limited by the computer precision and cannot be smaller than 10^{-15} (double precision). It is crucial to know the minimum size of the Krylov space needed to reach this precision for all requested eigenvalues. One can show that this minimum size n is sub-linear with respect to r (for the simple 2D model $\lambda_r = 1/r$) and the 2D simulations discussed below show that $n \lesssim 4r$.

4. Computations in 2D

4.1. The photonic crystal

In this section, we consider a 2D honeycomb lattice of infinite vertical rods. The 2D triangular lattice is generated by $a_1 = (\sqrt{3}/2, 1/2)$ and $a_2 = (\sqrt{3}/2, -1/2)$. The honeycomb lattice is obtained by centering two cylinders at $\frac{1}{3}(a_1 + a_2)$ and $-\frac{1}{3}(a_1 + a_2)$, respectively. The reciprocal lattice is generated by b_1 and b_2 such that $a_i \cdot b_j = \delta_{ij}$. The dielectric permittivity of the rods is set to $\epsilon = 5.36$ and the filling factor is set to 0.4. The corresponding control file to be used with the MIT Photonic-Bands (MPB) package [11] thus begins with:

```
(set!geometry-lattice (make lattice (size 1 1 no-size)
                      (basis1 (/ (sqrt 3) 2) 0.5)
                      (basis2 (/ (sqrt 3) 2) -0.5)))

(set!geometry
  (list
    (make cylinder
      (center (/3) (/3) 0) (radius 0.234803938515)
      (height infinity)
      (material (make dielectric (epsilon 5.36)))
    )

    (make cylinder
      (center (/-3) (/-3) 0) (radius 0.234803938515)
      (height infinity)
      (material (make dielectric (epsilon 5.36)))
    )
  )
)
```

We now present calculations of TM and TE modes and discuss the convergence of the eigenvalues with respect to the dimension n of the Krylov space (see Theorem 1).

4.2. Example of TM modes in the honeycomb lattice

As discussed above, the calculation of TM modes is simplified since the inversion of the Maxwell operator $\boldsymbol{\Theta}_k$ is straightforward. The standard Lánczos method may be applied: a Krylov space K is constructed by iteration of $\boldsymbol{\Theta}_k^{-1}$ applied to an initial magnetic field h. Then the matrix elements of $\boldsymbol{\Theta}_k^{-1}$ are computed in K.

Fig. 2 plots the relative errors for four eigenvalues $\lambda_1(n)$, $\lambda_2(n)$, $\lambda_4(n)$ and $\lambda_8(n)$ with respect to the dimension of the Krylov space which runs from $n = 8$ to $n = 30$. The Block vector is $k = 0.3b_1$. Notice that the largest eigenvalue λ_1 corresponds to the first mode of the Maxwell operator.

Corollary 1 shows that $|\frac{\mu}{\lambda_r} - 1| \leqslant \frac{\lambda_1}{\lambda_r} \tan \varphi_r \delta_r$. Thus, Fig. 2 should be similar to Fig. 1 up to the factor $\tan \varphi_r$. This factor must be much larger than 1 (at least for most eigenvalues). Thus, the values in Fig. 2 should be larger than in Fig. 1. At the opposite, the values in Fig. 2 are much smaller and the computer double precision is obtained for $n \approx 4r$, showing that the upper bounds of Fig. 1 are far from optimal. In fact Theorem 1 only provides upper bounds and the distribution of the largest eigenvalues certainly differs from the asymptotic free spectrum $\lambda_r = 1/r$.

Fig. 3 illustrates the convergence of $\lambda_6(n)$ as a function of the dimension of the Krylov space ($n = 8$ to $n = 21$) for three sizes 64×64, 256×256 and 1024×1024. The Block vector is $k = 0.3b_1$.

The roughness of the curves reflects the fluctuations of the calculated eigenvalues with respect to the initial conditions: each eigenvalue is computed with a different random initial magnetic field. As expected from Theorem 1 the convergence is independent of the size of the sample.

Fig. 4 plots the dispersion curves for the frequencies $\omega a/2\pi c = 1/(2\pi\sqrt{\lambda})$ of the six first modes of $\boldsymbol{\Theta}_k$ where k runs over the path $\{\Gamma, M, K, \Gamma\}$ of the Brillouin zone.

4.3. Example of TE modes in the honeycomb lattice

As mentioned in Section 3, the iteration of the inverse Maxwell operator $\boldsymbol{\Theta}_k^{-1}$ requires the inversion of the operator $\mathbf{A}_k = P_{\perp,k}\varepsilon^{-1}P_{\perp,k}$. An approximate inverse may be computed by a standard conjugate gradient method and the precision therefore depends on the number of performed steps. An approximate Krylov

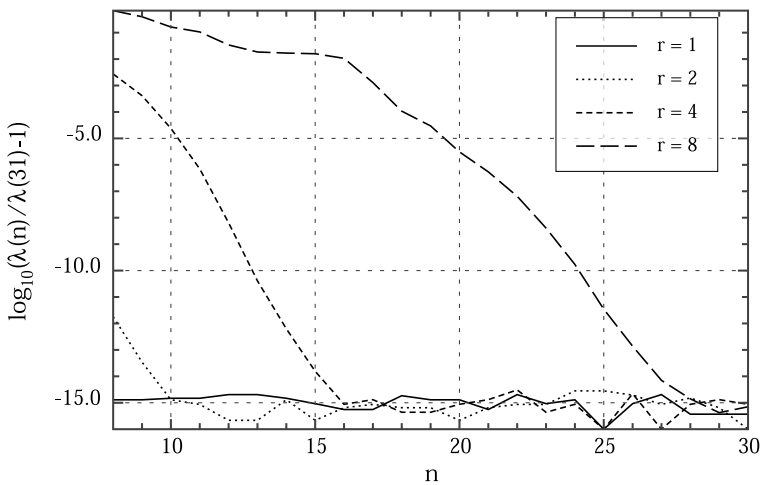

Fig. 2. TM modes. Relative errors for λ_1, λ_2, λ_4 and λ_8 as function of the dimension $n = 8, \ldots, 30$ of the Krylov space. The sample is 128×128.

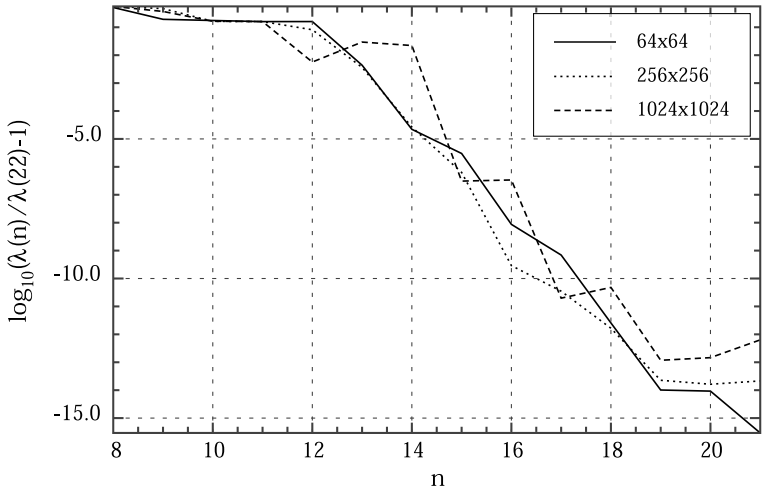

Fig. 3. TM modes. Relative errors for λ_6 as function of the dimension $n = 8, \ldots, 21$ of the Krylov space and for different sizes of the sample.

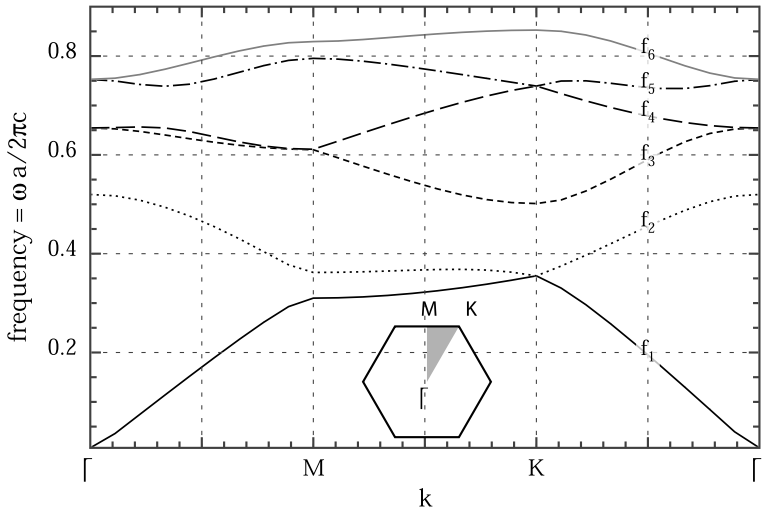

Fig. 4. TM modes. Frequencies of the first six modes. The dimension of the Krylov space is set to 20 and the size of the sample is 128×128.

space K is constructed by iteration of the approximate inverse of $\boldsymbol{\Theta}_k^{-1}$ applied to an initial magnetic field h. Then the exact matrix elements of $\boldsymbol{\Theta}_k$ are computed in K. A sketch of the algorithm is then:

Start with a random unit vector v_0 and assume that the approximate Krylov space K_m contains m vectors $v_0, \ldots, v_{m-1}$ such that $(v_i, v_j) = \delta_{ij}$. The next vector v_m is obtained by the following algorithm:

- compute $y_m = \mathbf{B}_k^{-1} v_{m-1}$,
- solve $\mathbf{A}_k x_m = y_m$ by some steps of conjugate gradient algorithm,

- compute $z_m = \mathbf{B}_k^{-1} x_m$,
- the space K_{m+1} is defined by the basis $\{v_0, \ldots, v_{m-1}, z_m\}$, and v_m is obtained by orthonormalization of this basis.

Finally, λ's are obtained as the inverse of the eigenvalues of the matrix $m_{ij} = (v_i, \boldsymbol{\Theta}_k v_j)$.

Fig. 5 displays the convergence of four eigenvalues $\lambda_1(n)$, $\lambda_2(n)$, $\lambda_4(n)$ and $\lambda_8(n)$, with respect to the dimension of the Krylov space which runs from $n = 8$ to $n = 30$. The size of the sample is 128×128 and the Block vector is $k = 0.3b_1$. The number of steps of the conjugate gradient algorithm is set to 6.

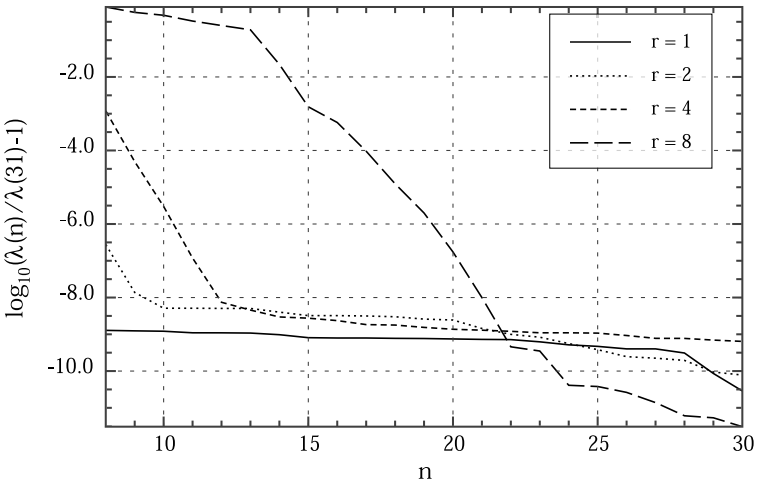

Fig. 5. TE modes. Relative errors for λ_1, λ_2, λ_4 and λ_8 as function of the dimension $n = 8, \ldots, 30$ of the Krylov space. The sample is 128×128 and the number of steps of the conjugate gradient algorithm is 6.

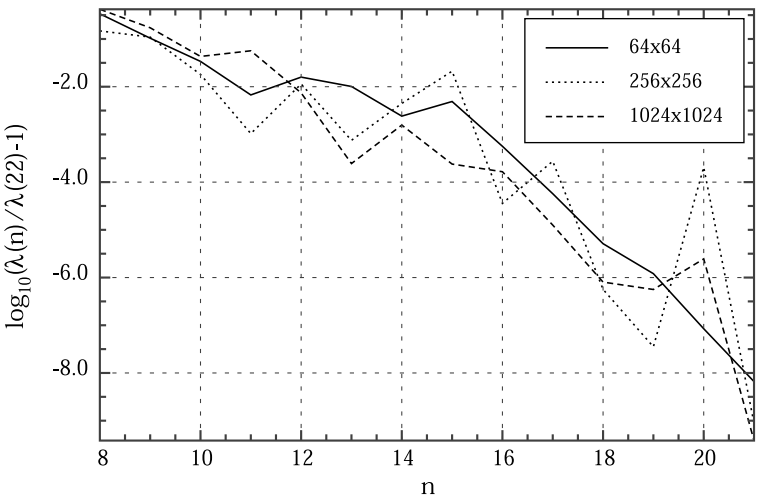

Fig. 6. TE modes. Relative errors for λ_6 as function of the dimension $n = 8, \ldots, 21$ of the Krylov space and for different sizes of the sample.

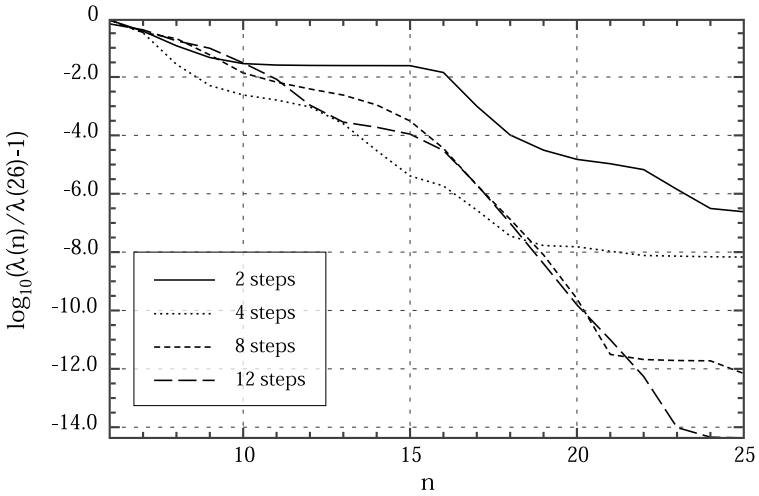

Fig. 7. TE modes. Relative errors for λ_6 as function of the dimension $n = 6, \ldots, 25$ of the Krylov space and for different number of steps in the conjugate gradient algorithm to compute $\mathbf{A}_k^{-1}$.

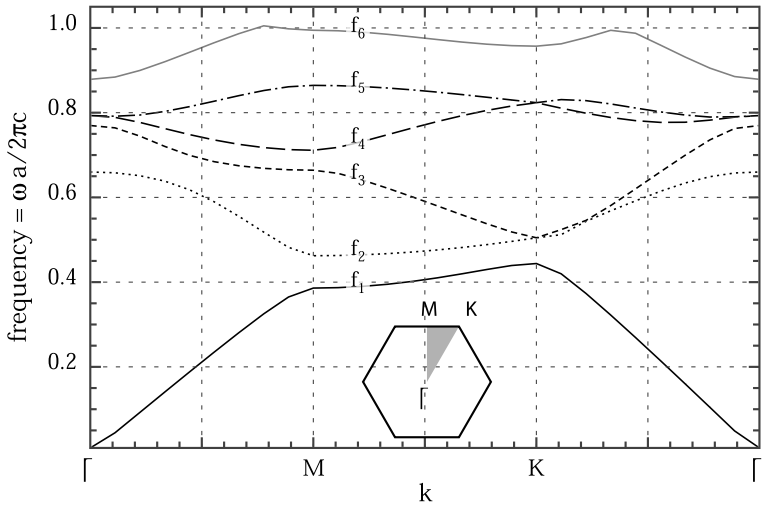

Fig. 8. TE modes. Frequencies of the first six modes. The dimension of the Krylov space is set to 20 and the size of the sample is 128×128. The number of steps of the conjugate gradient algorithm is 8.

Fig. 6 displays the convergence of $\lambda_6(n)$ as a function of the dimension of the Krylov space ($n = 8$ to $n = 21$) for three sizes 64×64, 256×256 and 1024×1024 of the sample. The Block vector is $k = 0.3b_1$ and the number of iterations of the conjugate gradient algorithm is 6. The random initial magnetic fields are different for each size and each n. As expected from Theorem 1, the convergence is independent of the size of the sample.

Fig. 7 illustrates the convergence of $\lambda_6(n)$ as a function of the dimension of the Krylov space ($n = 6$ to $n = 25$) for three different numbers of steps in the conjugate gradient algorithm (2, 4 and 8) for the computation of $\mathbf{A}_k^{-1}$.

As mentioned above for the TM modes, the optimal Krylov size $n \approx 4r$ seems correct.

Fig. 8 plots the dispersion curves for the frequencies $\omega a/2\pi c = 1/(2\pi\sqrt{\lambda})$ of the six first modes of $\boldsymbol{\Theta}_k$ where k runs over the path $\{\Gamma, M, K, \Gamma\}$ of the Brillouin zone.

5. Conclusion

We have shown that the Lánczos method applied to the inverse Maxwell operator provides a superconvergent algorithm for the computation of the lowest eigenmodes of the Maxwell operator in a periodic dielectric medium. This method may be extended to more general cases where one needs to compute the lowest eigenvalues of an unbounded operator with compact resolvent, for instance the one-electron Schrödinger operator with periodic potential.

References

[1] E. Yablonovitch, Inhibited spontaneaous emission in solid-state physics and electronics, Phys. Rev. Lett. 58 (1987) 2059.
[2] G.H. Golub, C.F. Van Loan, Matrix Computations, Johns Hopkins University Press, Baltimore, MD, 1996.
[3] B.N. Parlett, The Symmetric Eigenvalue Problem, Prentice-Hall, Englewood Cliffs, NJ, 1980.
[4] J.D. Joannopoulos, R.D. Meade, J.N. Winn, Photonic Crystals: Molding the Flow of Light, Princeton University Press, Princeton, NJ, 1995.
[5] S.G. Johnson, J.D. Joannopoulos, Photonic Crystals: the Road from Theory to Practice, Kluwer, Boston, 2002.
[6] Photonic Band Gap Links. Available from: <http://www.pbglink.com/index.html>.
[7] S.G. Johnson, J.D. Joannopoulos, Block-iterative frequency-domain methods for Maxwells equations in a planewave basis, Opt. Exp. 8 (3) (2001) 173.
[8] M. Duneau, F. Delyon, M. Audier, Holographic method for a direct growth of three-dimensional photonic crystals by chemical vapor deposition, J. Appl. Phys. 96 (5) (2004) 2428.
[9] M. Reed, B. Simon, Methods of Modern Mathematical Physics, IV: Analysis of Operators, Academic Press, London, 1978.
[10] C. Lánczos, An iteration method for the solution of the eigenvalue problem of linear differential and integral operators, J. Res. Nat. Bur. Stand. 45 (1950) 255.
[11] MIT Photonic-Bands. Available from: <http://ab-initio.mit.edu/mpb/>.